Extended MHD and Coupled Fluid-Kinetic Simulations of Planetary Magnetospheres: Applications to Mercury and Ganymede

Xianzhe Jia

With special thanks to Changkun Li, Hongyang Zhou, Yuxi Chen and Gabor Toth

University of Michigan

ISSS-15 / IPELS-16, August 5-9, 2024
IPP Garching, Germany

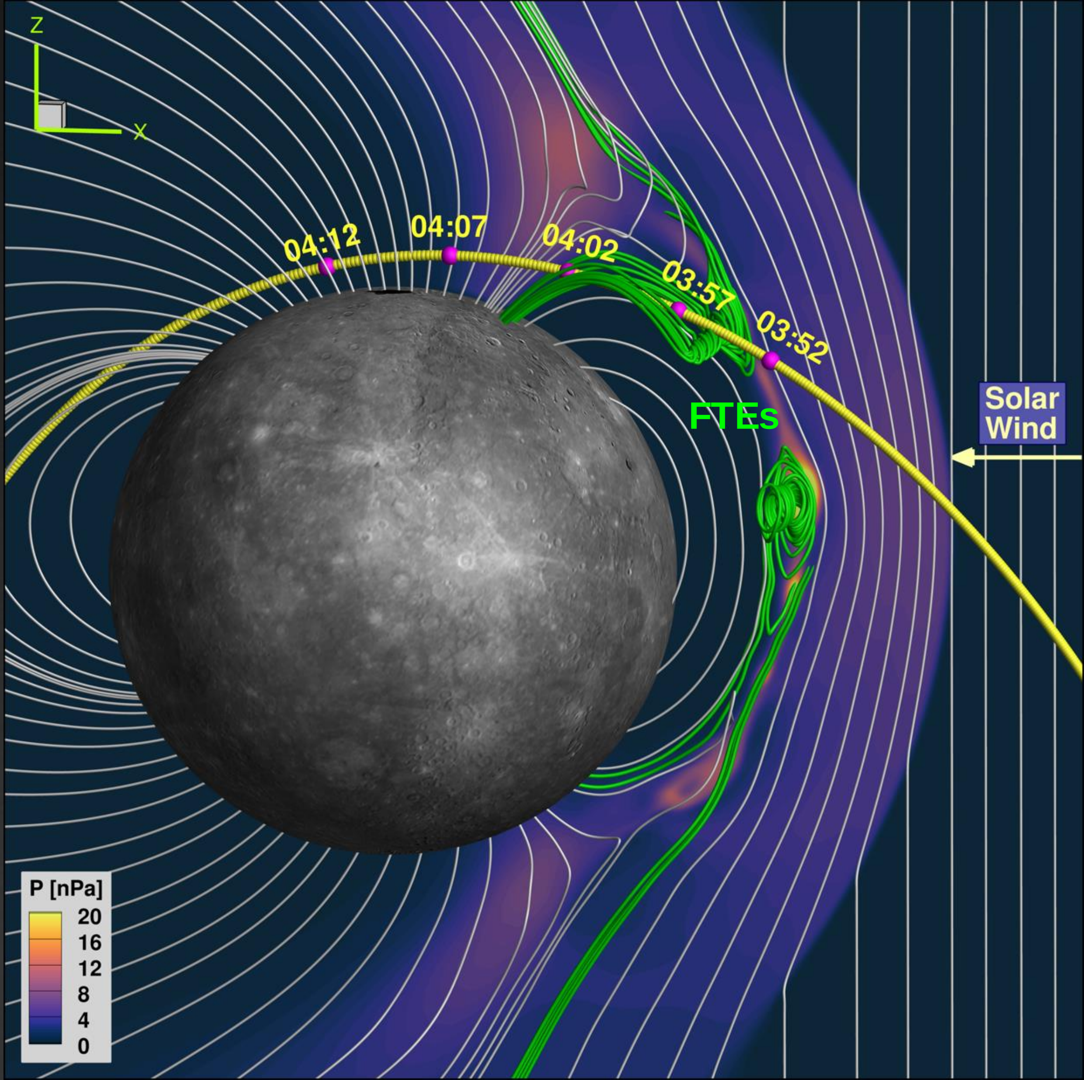

Space Weather Modeling Framework

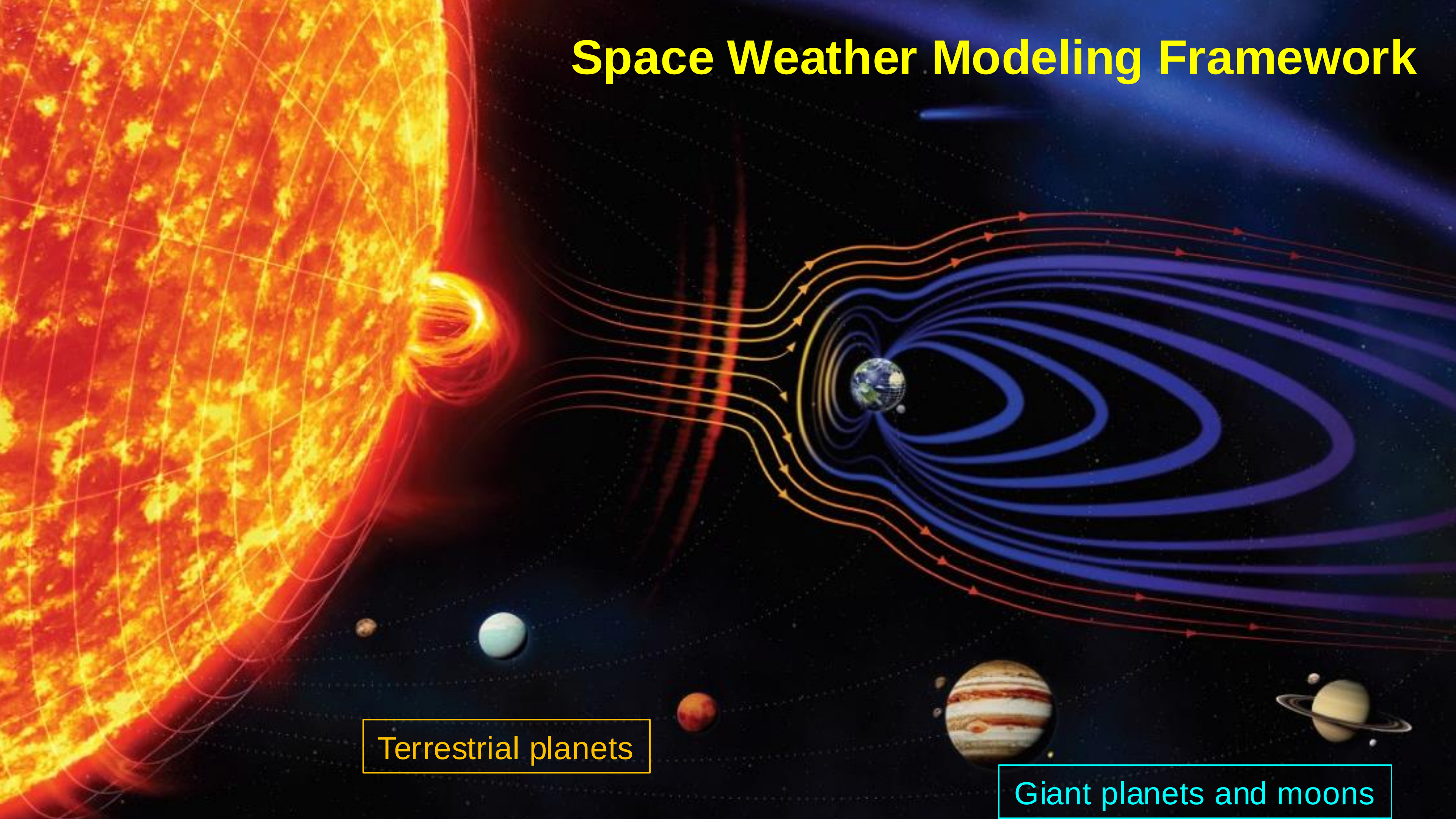

American Museum of Natural History – Hayden Planetarium Space Show VI

Worlds Beyond Earth

UMich Contributors: Yash Sarkango*, Camilla Harris*, Xianzhe Jia

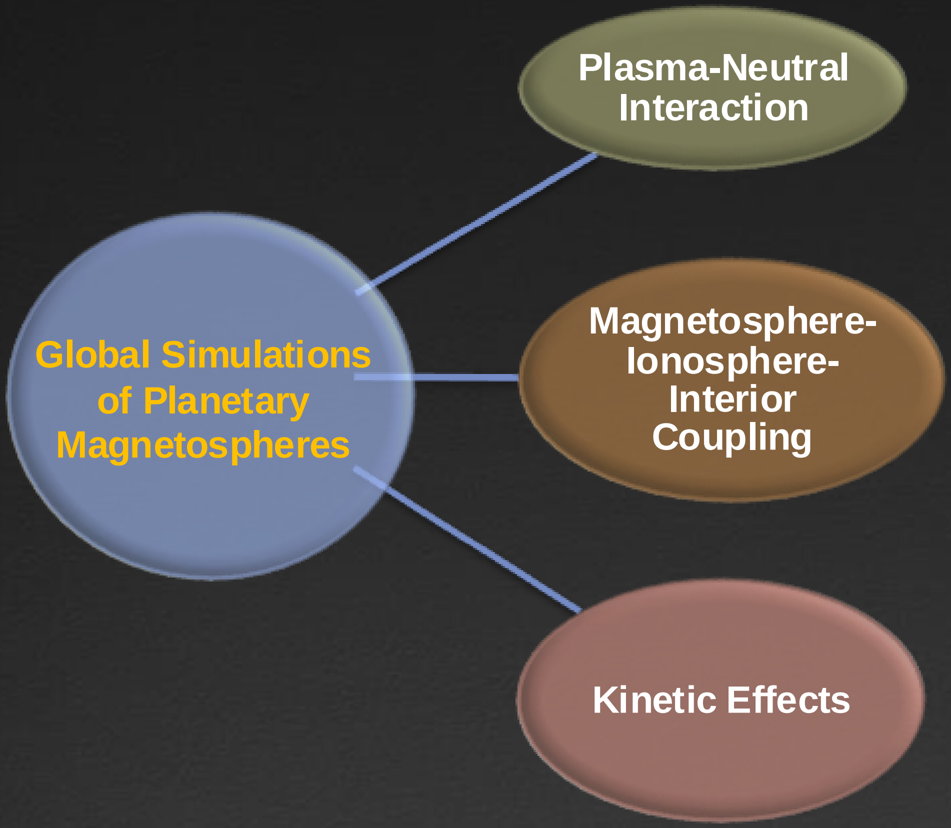

- Mass- and momentum loading
- Multiple ion and neutral species

Jupiter (Sarkango+2019), Saturn (Jia+2012a, b, c, 2016), Europa (Rubin+2015; Jia+2018; Harris+2021, 2022)

- Ionospheric properties (e.g., conductance, outflow)
- Interior/surface properties (e.g., induction effect)

Jupiter (Sarkango+2019), Saturn (Jia+2012a, b, c, 2016), Ganymede (Jia+2008, 2009; Zhou+2019, 2020), Mercury (Jia+2015, 2019)

- Magnetic reconnection
- Particle transport and energization

Ganymede (Toth+2016; Zhou+2019, 2020; Jia+2022), Mercury (Chen+2019; Li+2023, 2024) Saturn (Jia and Chen, in prep.)

Mercury's Magnetosphere

- Despite its relatively weak intrinsic field, Mercury has a well-developed magnetosphere with many familiar structures found in other planetary magnetospheres
  - Often considered as a "scaled-down version" of the Earth's magnetosphere

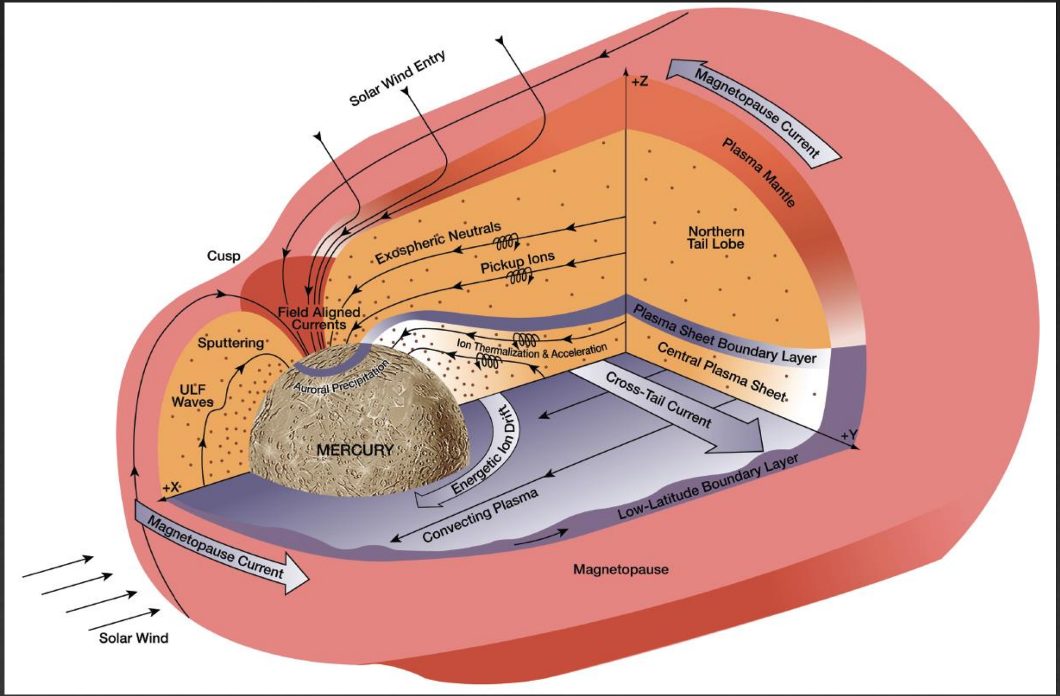

(*Slavin et al.*,2008)

Reconnection-driven Dynamics and FTEs at Mercury

- Located in the inner heliosphere, Mercury's magnetosphere routinely interacts with low Alfvénic Mach number solar wind, thereby making the dayside magnetopause very conducive to reconnection.

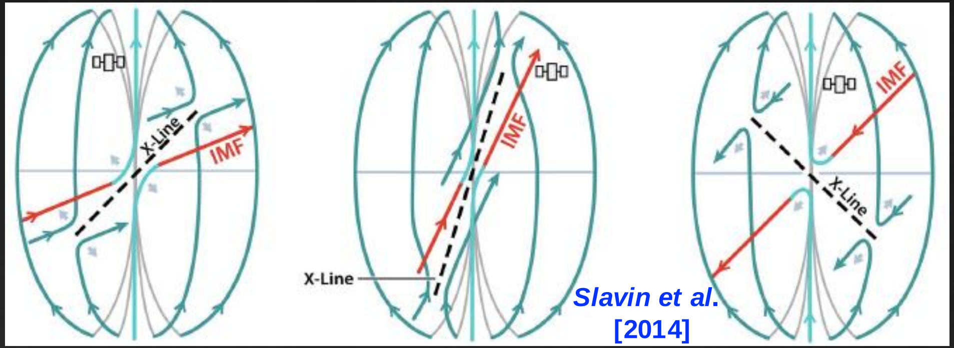

- As observed by MESSENGER, Mercury's magnetopause reconnection takes place under a wide range of IMF orientations, with frequent occurrence of FTEs as a results of multiple X-line reconnection (e.g., *Slavin et al*., [2012]).

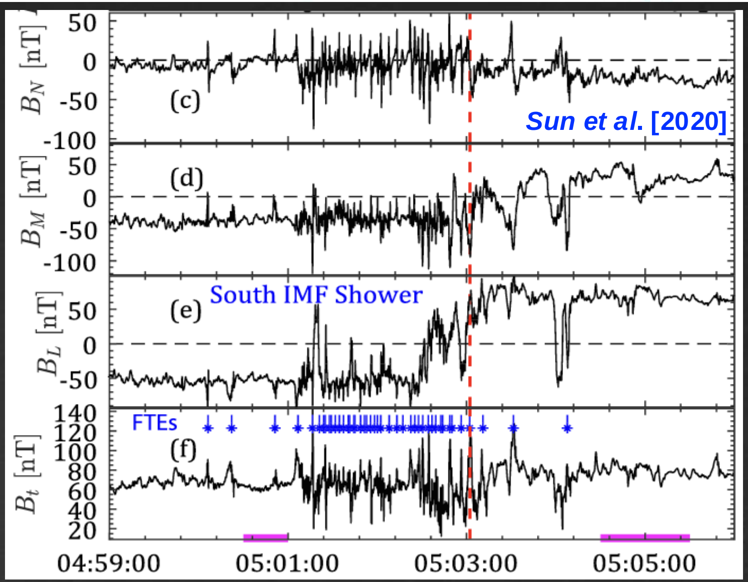

- FTEs play an important role in the solar wind-magnetosphere coupling at Mercury with significant contributions to the global mass and magnetic flux transport (e.g., *Imber et al*., 2014; *Fear et al*., 2019; *Sun et al*., 2020).

Global Hall-MHD Simulations of Mercury's Magnetosphere

- **BATSRUS Hall MHD model**
  - 3D global Hall MHD (*Toth et al.*, 2008)
  - Ohm's law: $\vec{E} = -\vec{u} \times \vec{B} + \frac{\vec{J}\times\vec{B}}{ne}$
  - AMR spherical grid with finest resolution near the dayside magnetopause: **20 km (0.008 R_M)** ~ 1/6 ion inertial length
  - Coupled planetary interior that captures the induction effects of Mercury's core (*Jia et al.*, 2015, 2019)

- **Steady upstream driving representing different solar wind M_A and IMF orientations.**

Run #	B_y (nT)	B_z (nT)	U_x (km/s)	n_{sw} (/cc)	Solar wind M_A	IMF clock angle (°)
1	0	-23	-500	36	6	180
2	-16	-16	-500	36	6	135
3	-23	0	-500	36	6	90
4	0	-69	-500	36	2	180
5	-49	-49	-500	36	2	135
6	-69	0	-500	36	2	90

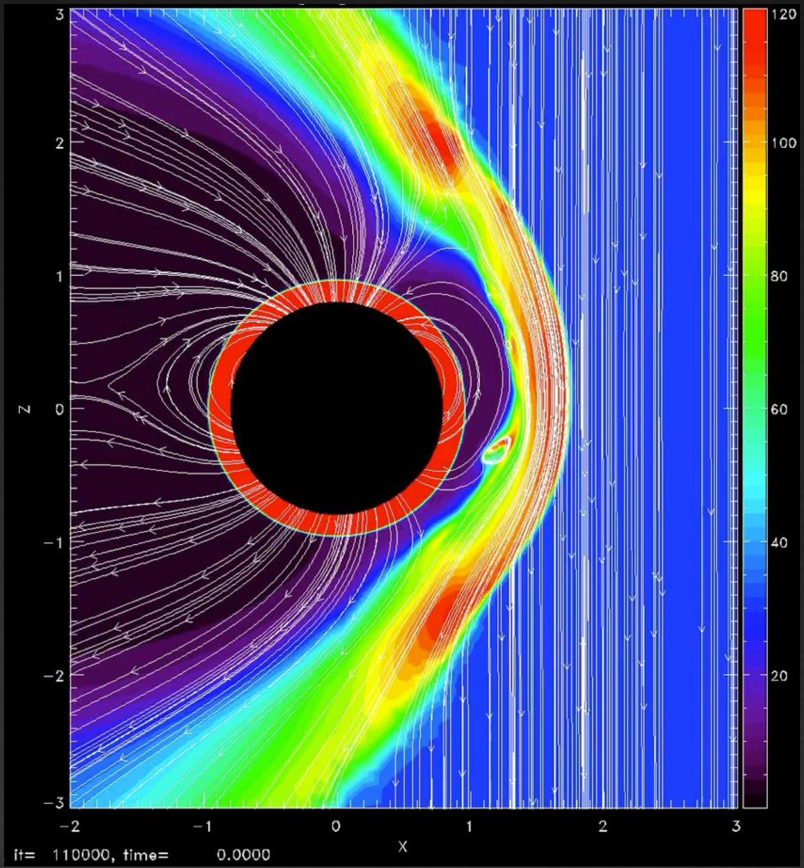

(*Li et al.*, JGR, 2023)

3D Magnetic Topology of FTEs

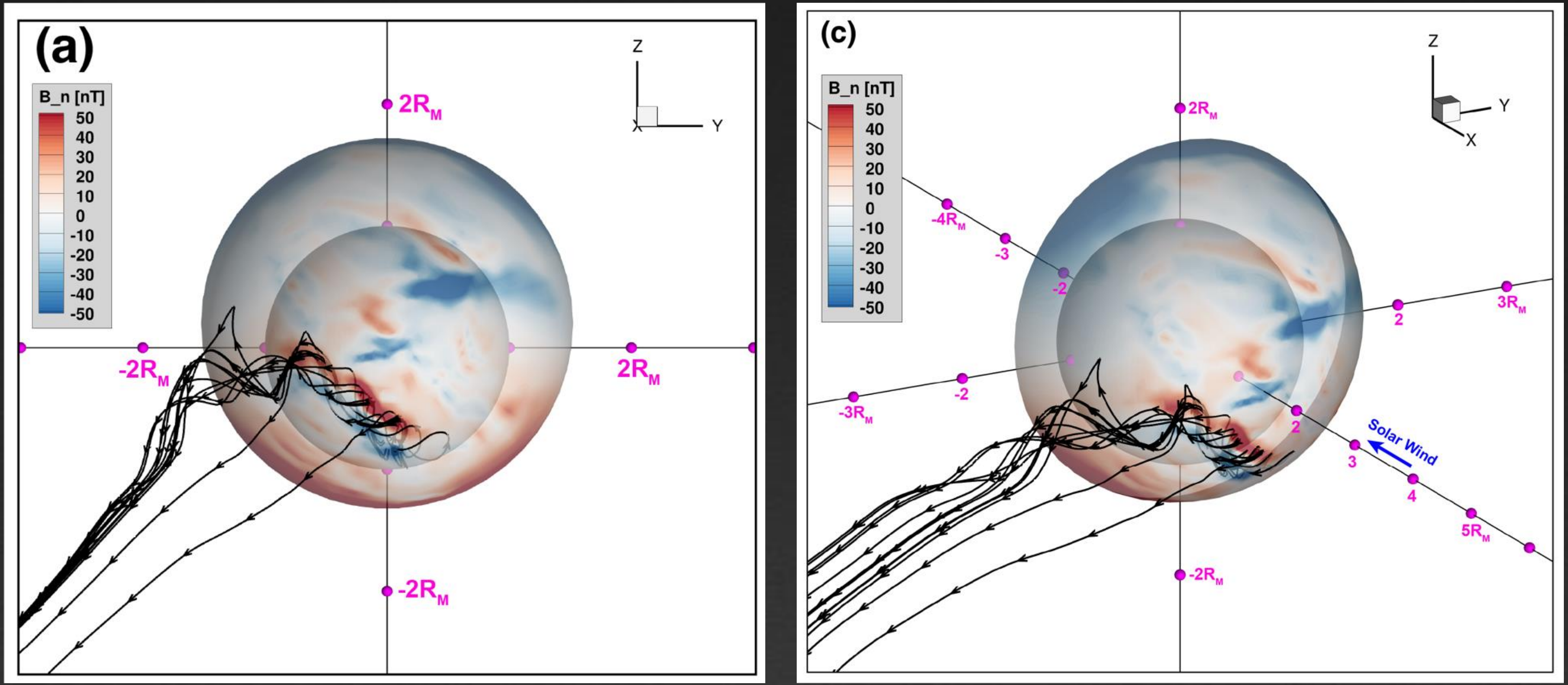

(*Li et al.*, JGR, 2023)

Quasi-periodic Occurrence of FTEs under Steady Upstream Driving

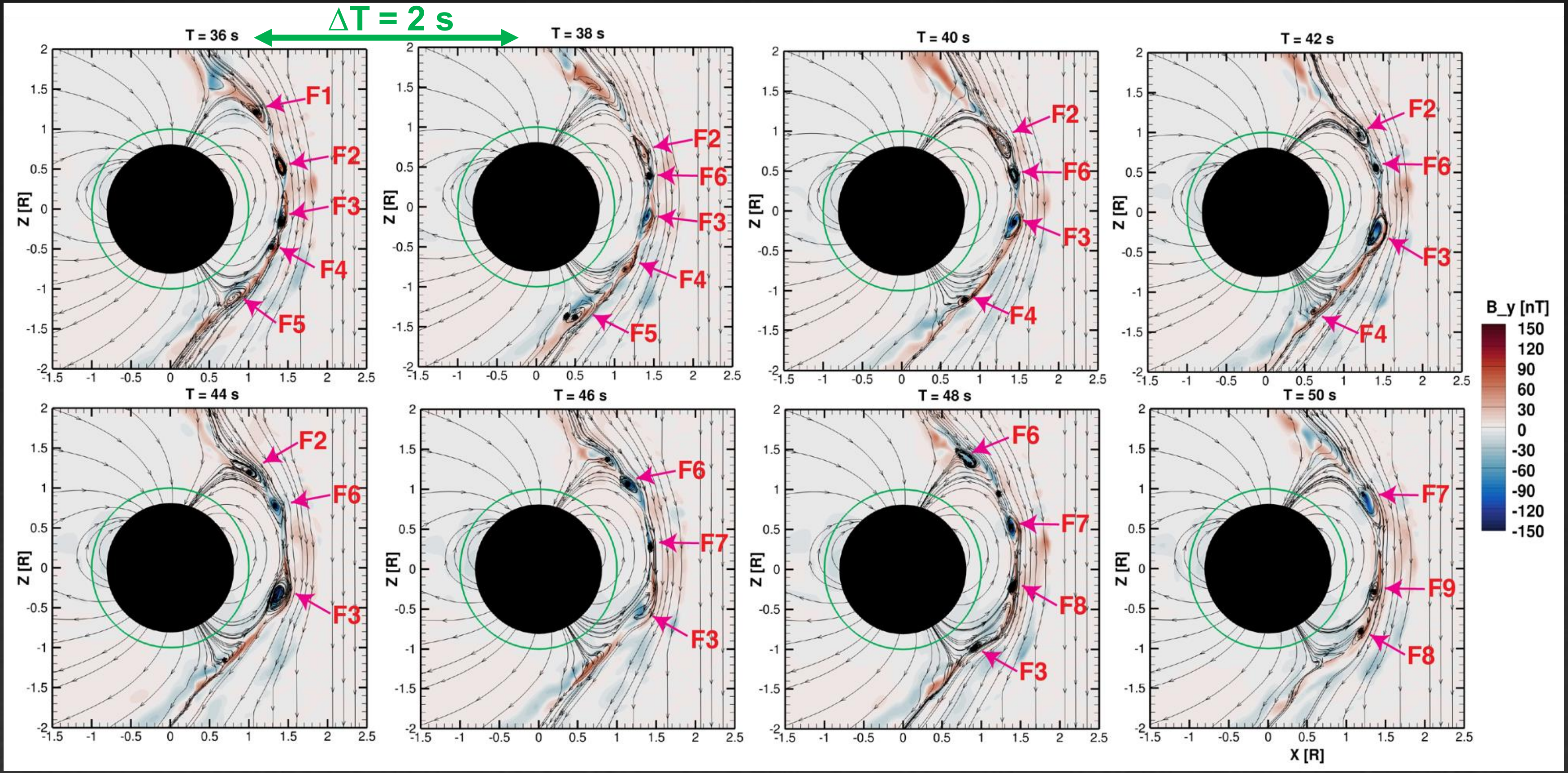

(*Li et al.*, JGR, 2023)

Tracking and Extracting FTEs in the Simulation

Dynamically fit simulated magnetopause with the *Shue et al.* (1997) empirical model

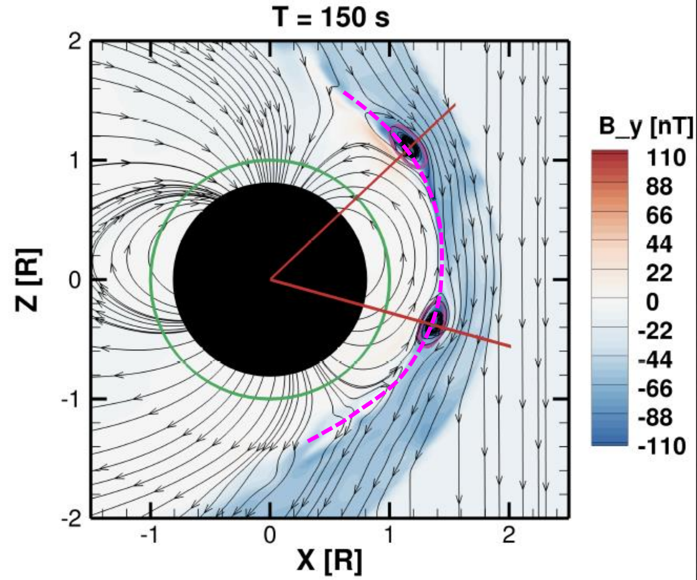

(*Li et al.*, JGR, 2023)

Latitude-time maps of extracted physical parameters on the magnetopause surface

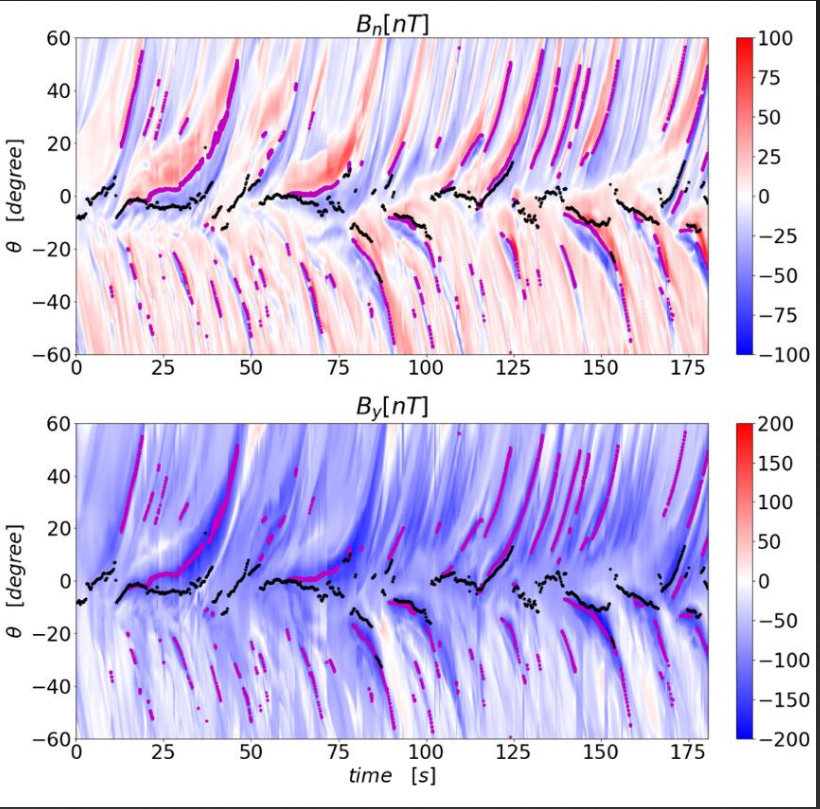

Statistics of Simulated FTEs and Dependence on Upstream Conditions

Solar Wind $M_A = 6$

Solar Wind $M_A = 2$

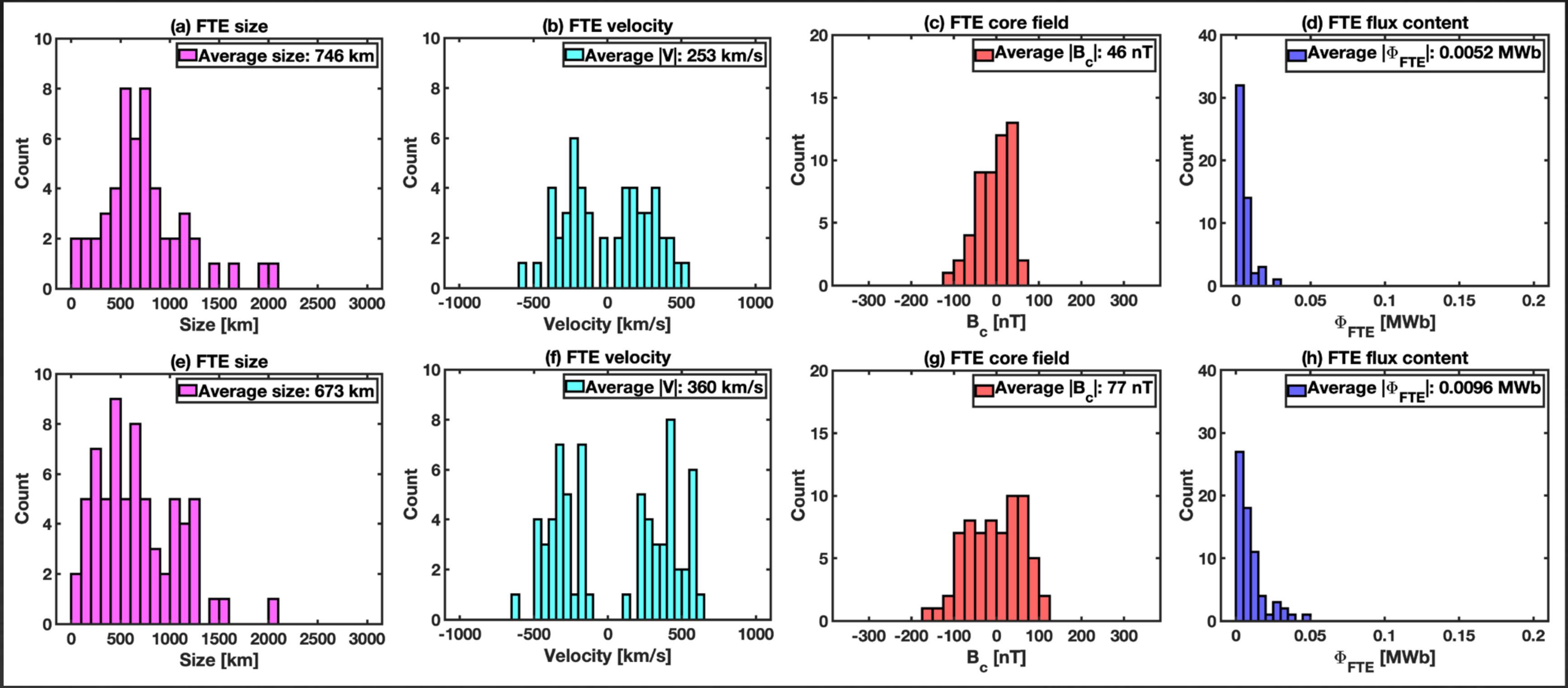

(*Li et al.*, *JGR*, 2023)

Coupled Fluid-Kinetic Simulations
- MHD with Adaptively Embedded PIC (MHD-AEPIC) -

(*Daldorff et al.*, 2014; *Toth et al.*, 2016; *Chen et al.*, 2017, 2019; *Zhou et al.*, 2019, 2020; *Wang et al.*, 2022, 2024; *Li et al.*, 2024)

Goal: Combine the efficiency of the global fluid code with the physics capabilities of the local PIC code

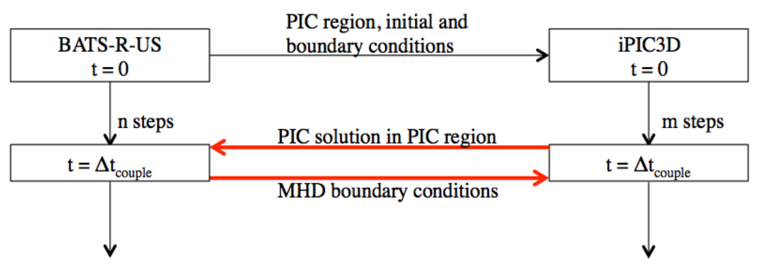

❖ **MHD code: BATSRUS** (*Powell et al.*, 1999)
- Time-dependent MHD (Hall, multi-fluid)
- Cartesian, spherical, cylindrical AMR grids

❖ **PIC codes: iPIC3D** (*Markidis et al.*, 2010) and **FLEKS** (*Chen et al.*, 2023)
- Solves full set of Maxwell's Equations implicitly on 3D Cartesian grid
- Both ions and electrons are treated kinetically
- Energy-conserving scheme (*Chen and Toth*, 2019)
- Cartesian grid with adaptive mesh refinement (*Chen et al.*, 2023)

❖ **Framework: SWMF** (*Toth et al.*, 2005, 2012; *Gombosi et al.*, 2023)
- Efficient two-way coupler developed for MHD-EPIC algorithm
- AEPIC allows multiple PIC regions with curved boundaries in the simulation domain

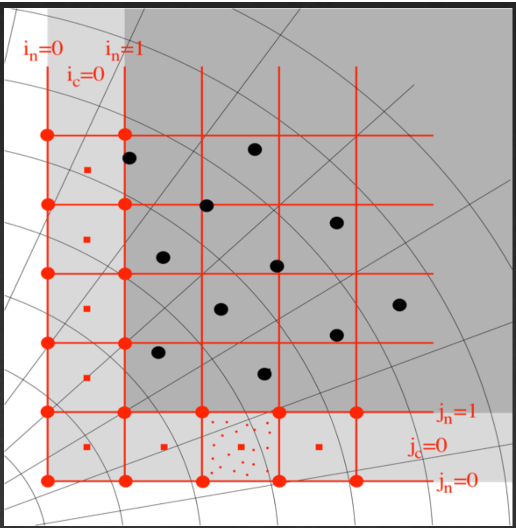

Darldorff et al. (2014)

MHD-AEPIC Simulations of Mercury's Magnetosphere

(*Li et al*., JGR, 2024)

Hall-MHD grid

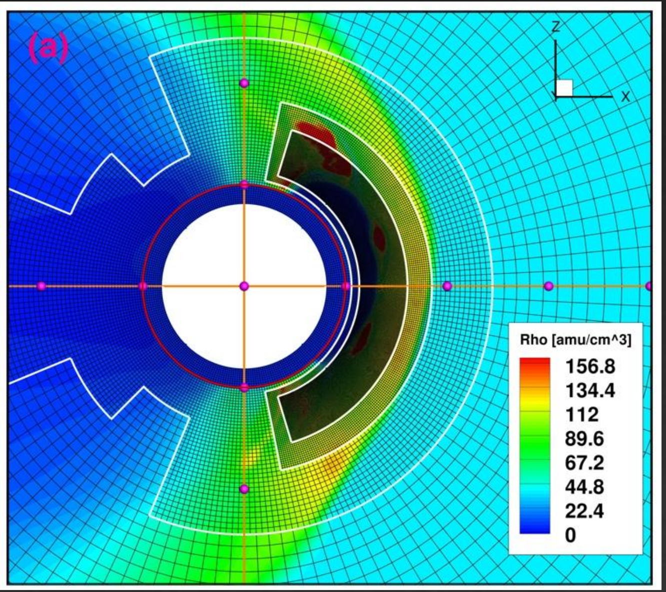

Spherical grid with multi-level refinement (grid resolution at the magnetopause: 20 km or 0.008 R_M)

Noon-midnight meridian | **Equatorial plane**

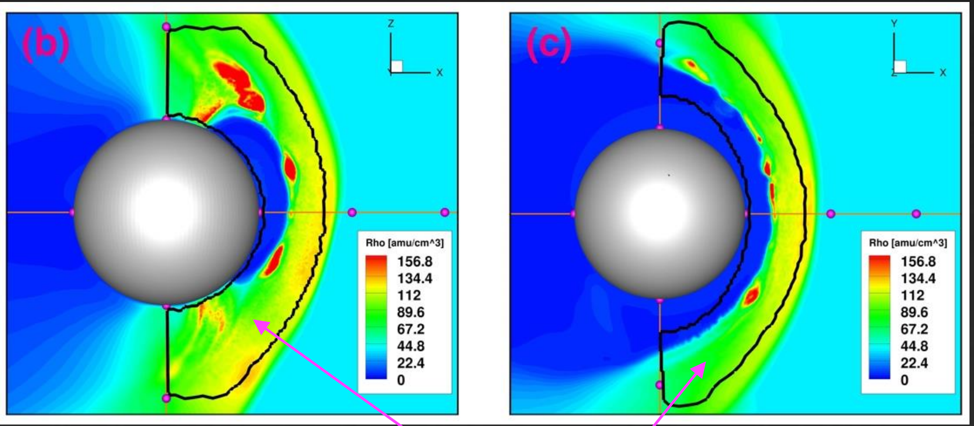

PIC region covering the entire dayside magnetosphere
(m_p/m_e = 100; 128 macro particles/cell)

Phase-space Distributions from PIC

(*Li et al.*, JGR, 2024)

Near Magnetopause X-line

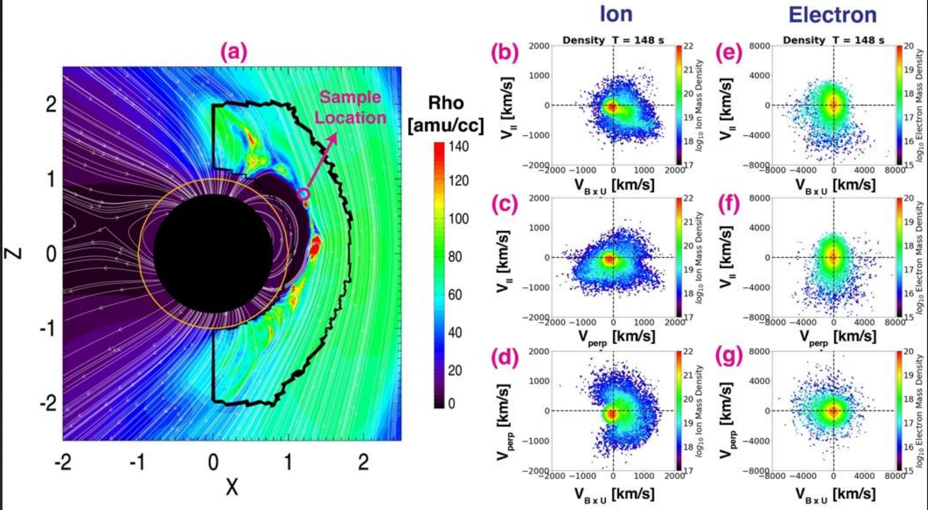

Southern Cusp

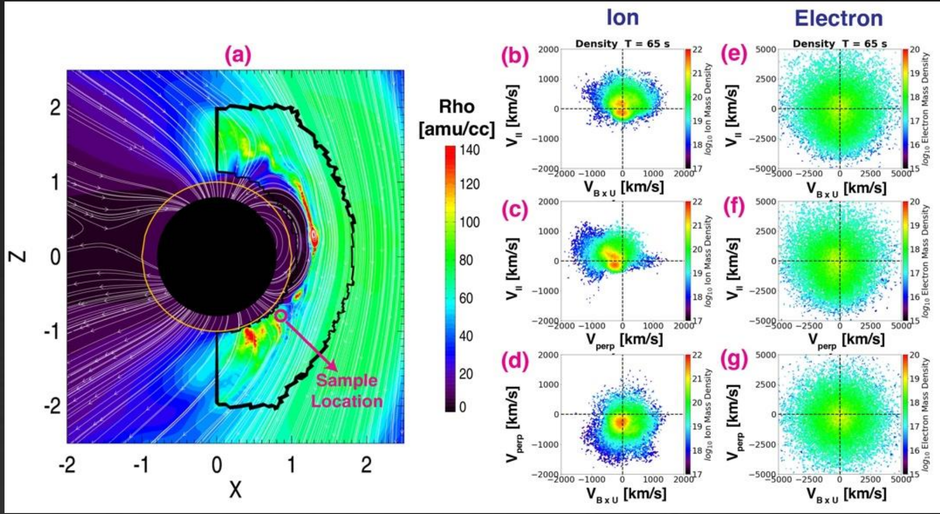

- Both the ion and electron distributions show strong deviations from Maxwellian near X-line.
- Crescent-shape ion distribution in the plane perpendicular to the local magnetic field.
- Strong anisotropy in the electron distribution with $T_{||} > T_{\perp}$

- Both precipitating and mirrored ion populations seen in the cusp.
- Electron distribution is approximately isotropic.

An Automated Method for Identifying X-lines in PIC

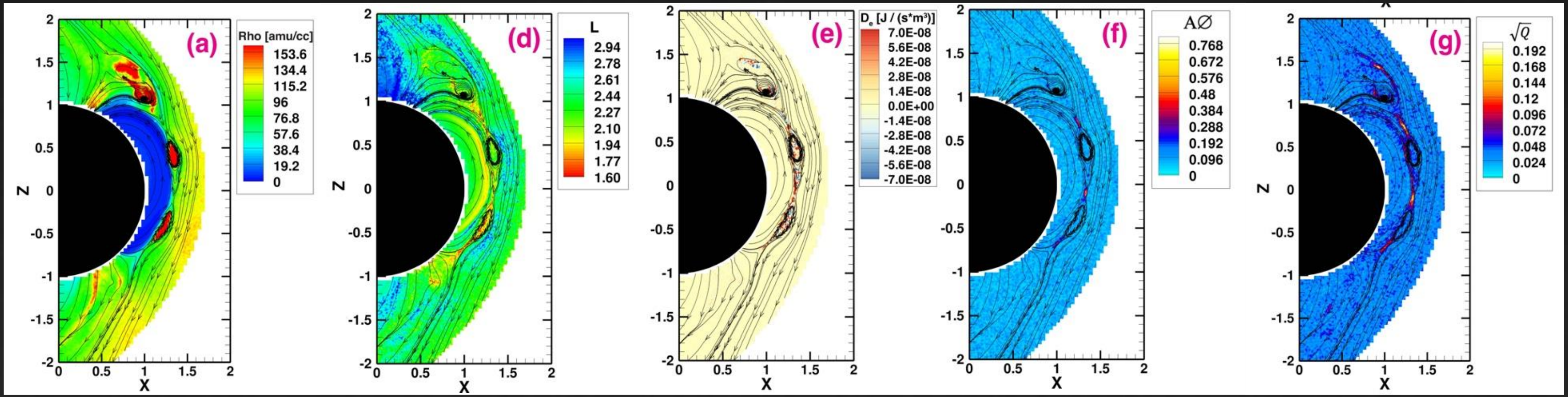

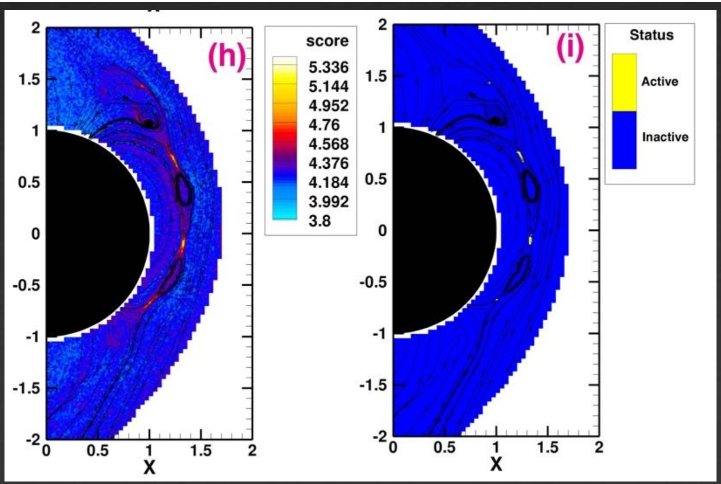

- Identify reconnection sites based on electron non-gyrotropy and non-ideal electric field.
- The automated algorithm works robustly for all MHD-AEPIC simulations with a wide range of upstream conditions.

3D Geometry of Magnetopause X-lines and FTEs

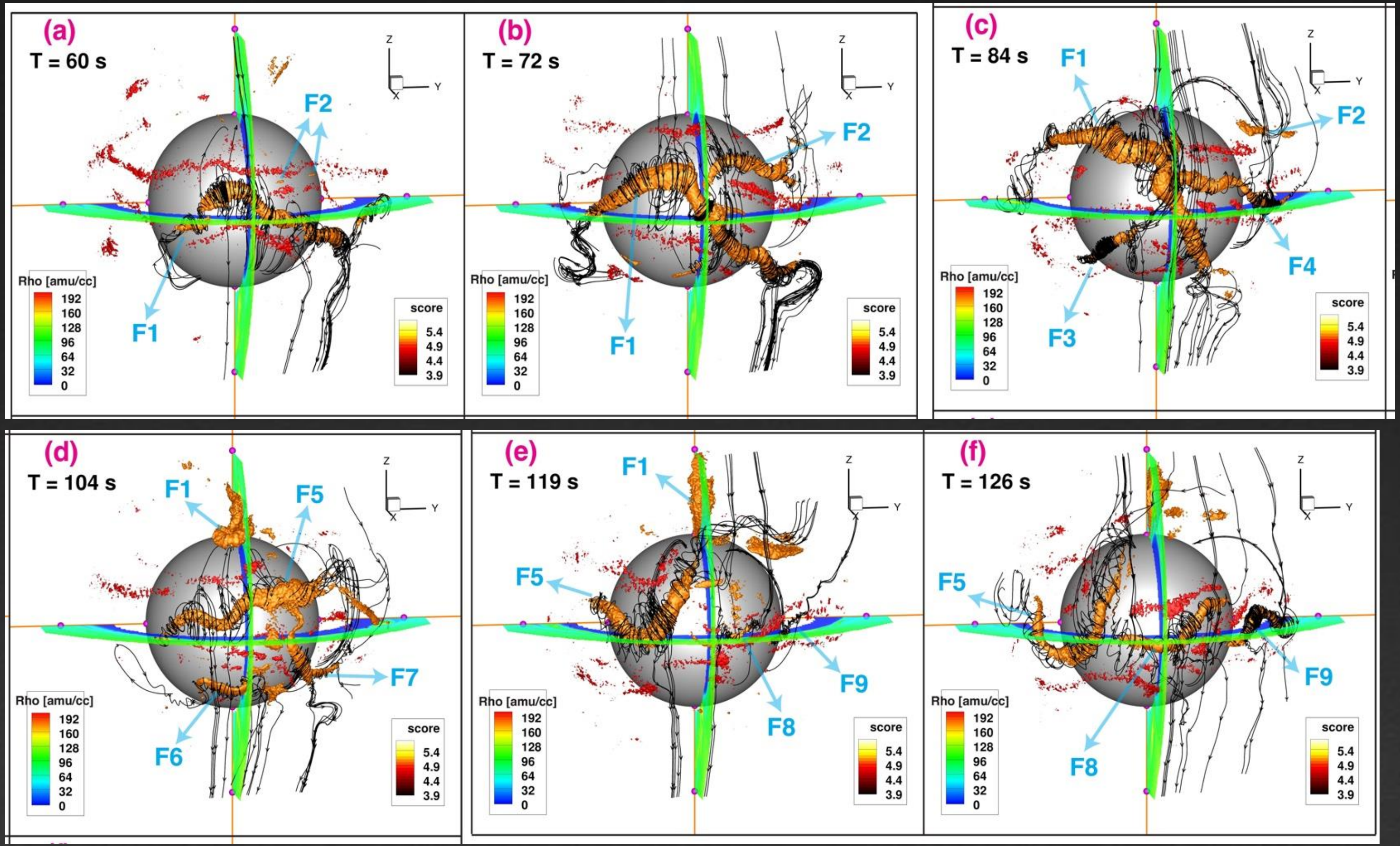

Dawn-dusk Asymmetry in Magnetopause Reconnection

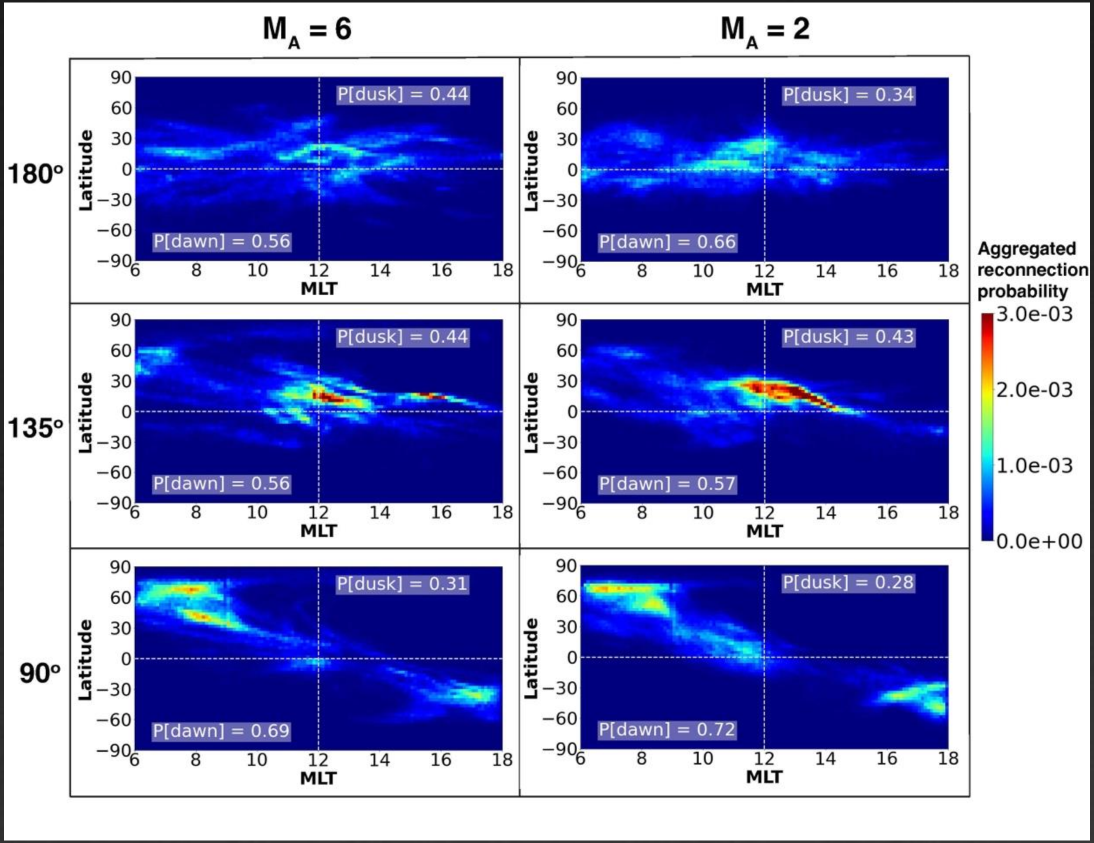

(*Li et al.*, JGR, 2024)

- Occurrence of magnetopause reconnection exhibits noticeable asymmetry, with the dawnside more favorable even under symmetric upstream conditions.
- The asymmetry becomes more pronounced for lower Mach number solar wind and IMF with stronger B_y.
- Potential mechanisms for asymmetry include X-line spreading (towards dawn) and suppression of reconnection due to Hall effects (towards dusk).

Statistics of Simulated FTEs (Hall-MHD vs MHD-AEPIC)

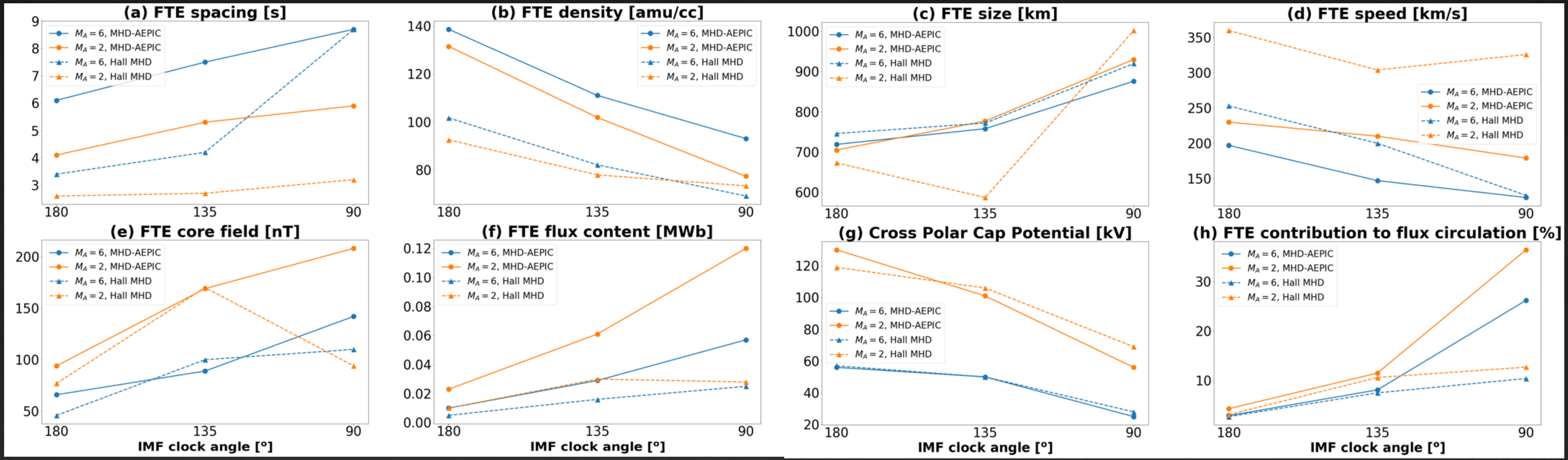

(*Li et al.*, JGR, 2024)

- FTE characteristics exhibit clear dependences on the upstream solar wind M_A and IMF orientation.
- Some quantitative differences between the two models: FTE occurrence rate, traveling speed and FTE flux content.
- Overall trends are very similar between Hall-MHD and MHD-AEPIC simulations using the same upstream conditions.

Jupiter's moon: Ganymede

– Strongly magnetized moon with its own magnetosphere –

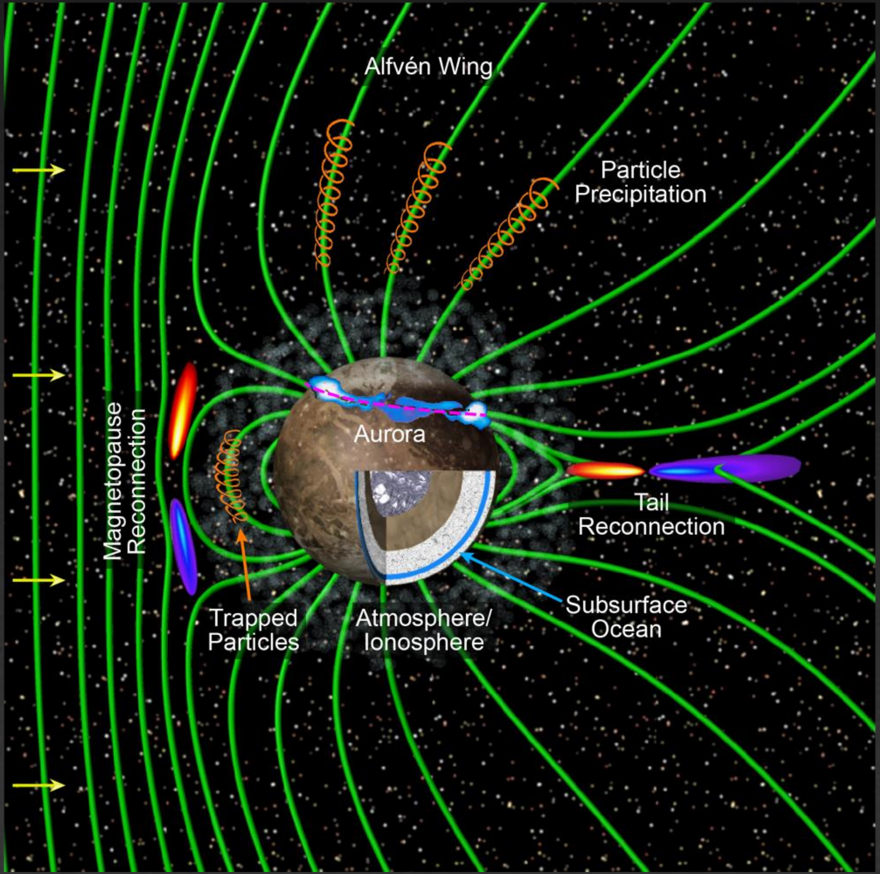

(Jia and Kivelson, 2021)

MHD-EPIC Simulations of Ganymede's Magnetosphere

❖ First application to Ganymede by *Toth et al.* (2016)
  ➢ 4 PIC regions covering both the upstream magnetopause and downstream tail
  ➢ Cartesian mesh for MHD + Cartesian grid for PIC

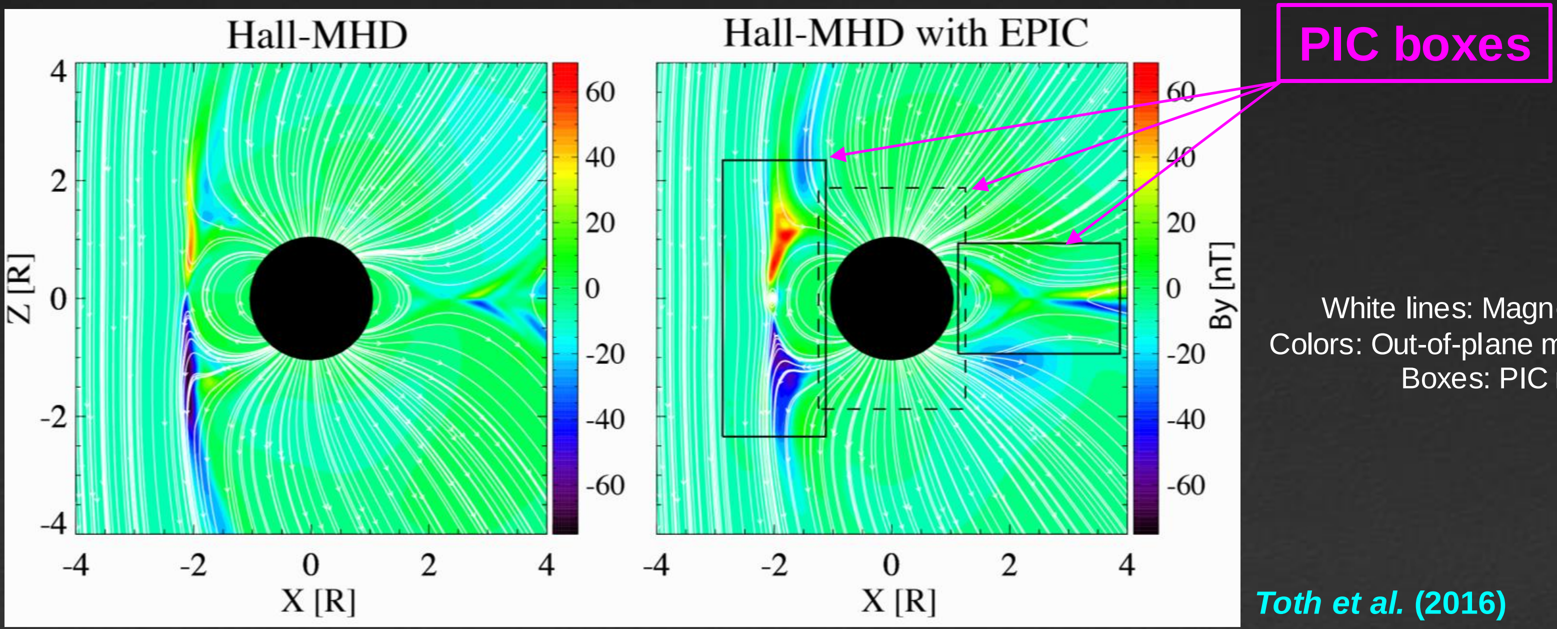

White lines: Magnetic field lines
Colors: Out-of-plane magnetic field (*By*)
Boxes: PIC regions

Toth et al. (2016)

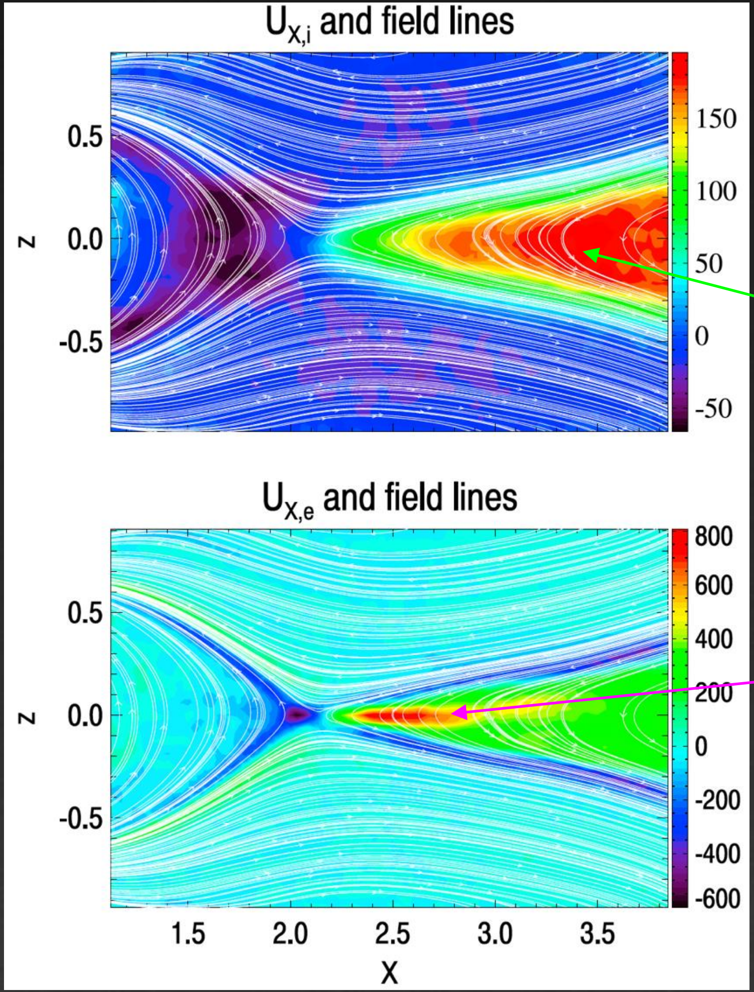

PIC-simulated Tail Reconnection

Ion jets

Electron jets

(*Toth et al.*, 2016)

Improved MHD-EPIC Simulations for Ganymede

- Upgraded model for Ganymede by *Zhou et al*. (2019)
  - Energy-conserving scheme
  - Coupled interior (*Jia et al.*, 2009)
  - Spherical mesh for MHD + Cartesian grid for PIC

	Hall MHD Spherical Grid	PIC Cartesian Grid	
Zhou+ 2019	0.1 d_I, 6 M cells	0.2 d_I, 0.6 M cells	0.15 billion particles
Zhou+ 2020	0.05 d_I, 27 M cells	0.1 d_I, 2.5 M cells	0.6 billion particles
$m_I / m_e = 100$, $d_I / d_e = 10$			

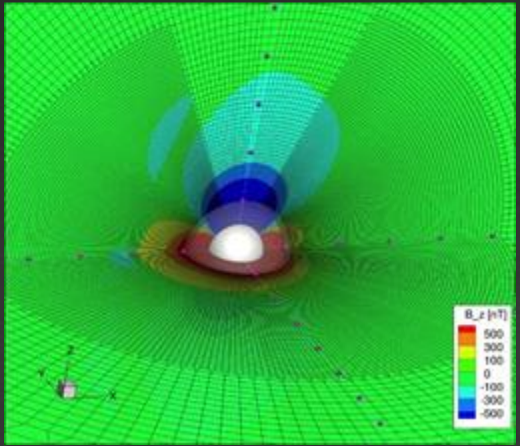

Comp. with Galileo data

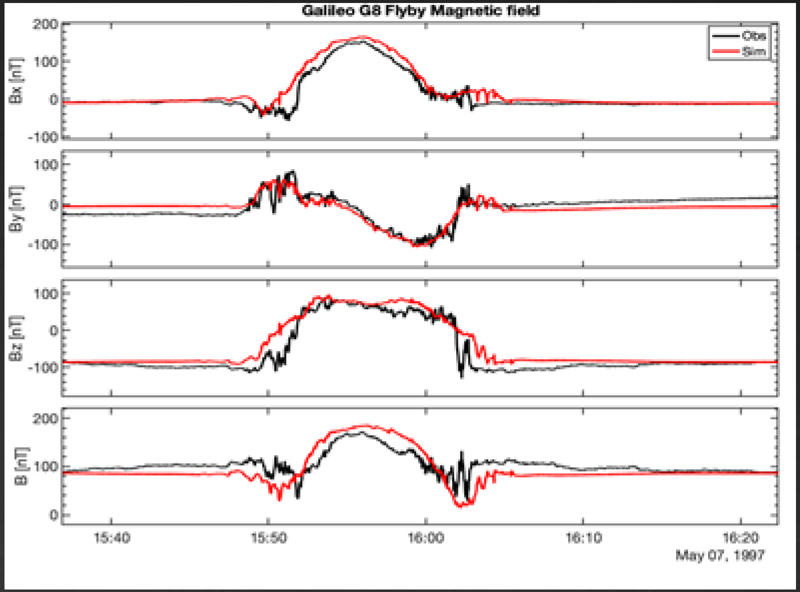

Ganymede's Magnetopause Reconnection in PIC

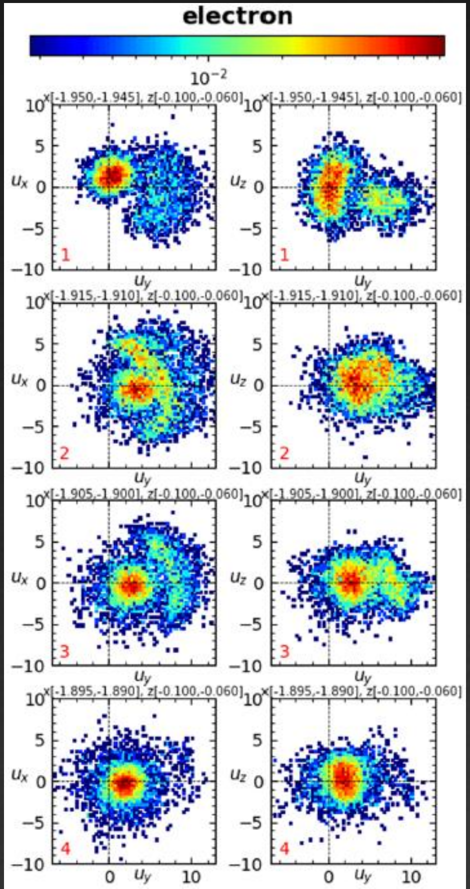

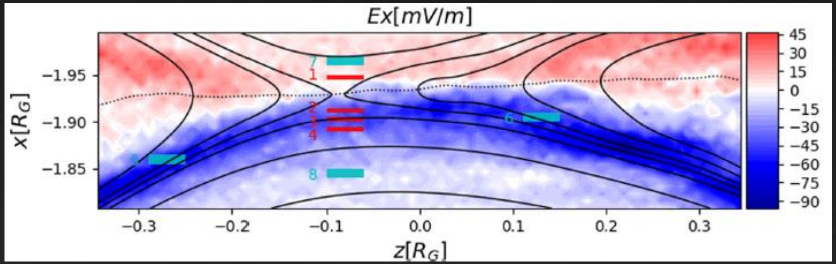

Zhou et al. (2020)

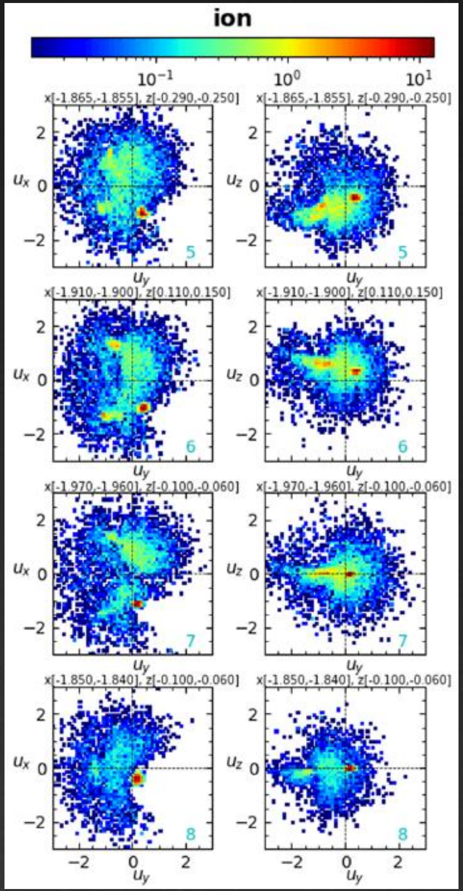

- Both ion and electron distributions near the reconnection X-line deviate strongly from Maxwellian.
- Crescent-shaped distributions are present in the inflow region of the diffusion region.
- Strong temperature anisotropies are found in the reconnection outflow region.

Summary

- Global simulations for planetary magnetospheres and their moons in recent years have gone beyond single-fluid MHD approach to include important physics that arises from non-ideal MHD effects and kinetic processes.

- Extended MHD and coupled fluid-kinetic models provide novel capabilities for resolving kinetic physics in a global system.
  - Applications of these models to Mercury and Ganymede have yielded new insights into the nature of magnetopause reconnection and its role in driving the global circulation of plasma and magnetic flux under different external conditions.

- MHD-EPIC simulations of the outer planet magnetospheres are currently under way to enable a better understanding of the solar wind-magnetosphere coupling and magnetospheric dynamics that operate under external and internal conditions drastically different from those at the inner planets.